Universality of the metal-insulator transition in three-dimensional disordered systems

J. Brndiar and P. Markoš
Institute of Physics, Slovak Academy of Sciences, 845 11 Bratislava, Slovakia

The universality of the metal-insulator transition in three-dimensional disordered system is confirmed by numerical analysis of the scaling properties of the electronic wave functions. We prove that the critical exponent ν and the multifractal dimensions d_q are independent on the microscopic definition of the disorder and universal along the critical line which separates the metallic and the insulating regime.

PACS numbers: 73.23.-b, 71.30., 72.10. -d

One of the main problem of the disorder induced metal-insulator transition (MIT) is the proof of its universality. In the pioneering work [1], it was conjectured that if the sample size exceeds all the length parameters of the model, then the conductance, g, is the only parameter which governs MIT. This scaling hypothesis has been confirmed by various numerical analysis, with the help of the finite-size scaling [2, 3].

Generally accepted scenario of the Anderson localization is that disorder broadens the conductance band. Electron states in the tail of the band become localized, separated from delocalized (metallic) states by the mobility edges, E_c. System exhibits the MIT if the Fermi energy, E_F, crosses the mobility edge. With increased disorder, E_c moves towards the band center. There is a critical value of the disorder, W_c, for which E_c reaches band center, $E_c = 0$. For disorder $W > W_c$, all electronic states inside the band become localized. Phase diagram in the energy-disorder plane was calculated in [4] and is schematically shown in the upper panel of Fig. 1.

At the band center, $E = 0$, the universality of the MIT was confirmed by detailed numerical analysis of the disorder and system size dependence of Lyapunov exponents in quasi-one dimensional systems [3, 5], mean conductance [6], conductance distribution [7], and level statistics [8, 9]. These studies determined the value of the critical exponent ν, which determines the divergence of the correlation length, $\xi \sim |W - W_c|^{-\nu}$, as $\nu = 1.57 \pm 0.02$ [5, 6]. The analysis of MIT along the critical line (non-zero energy E) is more difficult because the critical region is narrower and finite size effects are stronger [10]. Critical exponent, ν, was obtained only in models with random hopping [11], and very recently in [12].

In this paper, we present numerical proof of the universality of MIT. By scaling analysis of the electronic wave functions in the vicinity of two critical points, shown in the upper panel of Fig. 1, we prove that the critical exponent ν and fractal dimensions d_q of the wave function (defined below) are universal along the critical line.

Electron eigenenergies and wave functions are calculated for three-dimensional Anderson Hamiltonian,

$$\mathcal{H} = W \sum_r \epsilon_r c_r^\dagger c_r + \sum_{[rr']} c_r^\dagger c_{r'}. \qquad (1)$$

Here, r counts the sites of the three-dimensional (3D) lattice of the size L^3, ϵ_r is the random energy distributed either with the Box distribution, $P_B(\epsilon) = (2/W)\Theta(W/2 - |\epsilon|)$ or with the Gaussian distribution, $P_G(\epsilon) = \sqrt{2\pi W^2}\exp -(\epsilon^2/2W^2)$. Parameter W measures the strength of the disorder. For $E = 0$, the critical disorder $W_c \approx 16.5$ (6.15) for the Box (Gauss) distribution of random energies, respectively.

The quantities of interest are inverse participation ratios (IPR), $I_q(E_n)$. By definition, [13]

$$I_q(E_n) = \sum_r |\Phi_n(r)|^{2q}. \qquad (2)$$

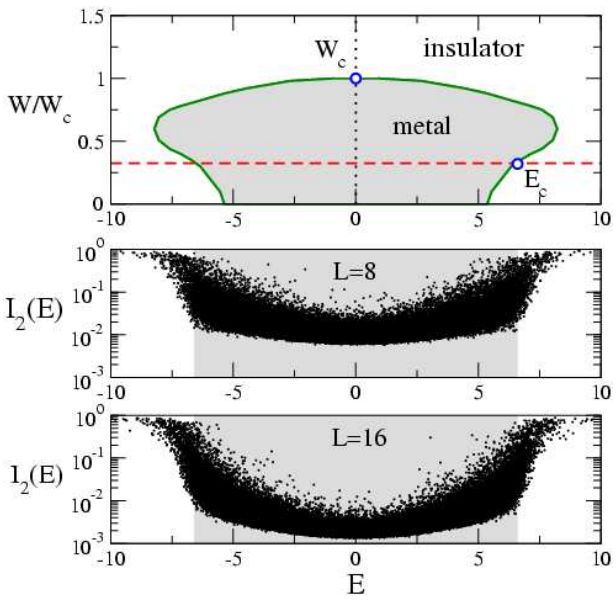

FIG. 1: (Color online) :w Top panel shows schematic phase diagram for 3D Anderson model. Solid line separates metallic (shaded area) and localized states. Open circles shows the position of critical points studied in this paper. Note that the mobility edge, E_c lies outside the unperturbed energy band. Two bottom panels present numerical data for I_2, given by Eq. (2) for cubes of the size $L = 8$ (middle) and $L = 16$ (bottom) and with Gaussian disorder $W = 2 = 0.325\ W_c$. In the metallic region, I_2 decreases when L increases, while I_2 becomes L-independent in the tail of the band, where electronic states are localized.

Here, E_n and $\Phi_n(r)$ is the nth eigenenergy and eigenfunction of the Hamiltonian (1), respectively.

The size dependence of IPR indicates the character of the eigenstate. If the nth eigenstate is conductive, the wave function is distributed throughout the sample and $|\Phi_n(r)| \propto L^{-d/2}$. Inserting in Eq. (2) we obtain that $I_q(E_n) \propto L^{d(1-q)}$. For localized state, $\Phi_n(r)$ is nonzero only in a small region, where $|\Phi_n(r)| \sim 1$. Hence, $I_q(E_n) \sim 1$, too. These size dependences are shown in two bottom panels of Fig. 1.

Different size dependence of $I_q(E)$ enables us to use IPR as a scaling variable for the calculation of the critical parameters in the same way as Lyapunov exponents [3], the conductance [6], or level statistics [8]. However, in contrast to the Lyapunov exponent or mean conductance, IPR is not a size independent constant at the critical point, but decreases as [14, 15, 16]

$$I_q(E = E_c) \sim L^{-d_q}, \tag{3}$$

where d_q are fractal dimensions. This makes the scaling analysis slightly more difficult. On the other hand, fractal dimensions, d_q, represent a new set of parameters, which can be used for the verification of the universality of the MIT. We expect that d_q are universal constants for all critical points along the critical line.

The energy spectrum of the Hamiltonian depends on the system size, L, and on the microscopic details of the disorder in a given sample. Therefore, we have to calculate an average values, defined as follows. For each system size, we consider a statistical ensemble of N_s samples which differ only in the realization of random energies, ϵ_r. For each sample, we calculate all eigenenergies, E_n, lying in a narrow energy interval, $E - \delta, E + \delta$, and calculate corresponding $I_q(E_n)$. For the ith sample, the number of eigenstates, n_i, depends on the microscopic realization of the disorder. Also, since the values of I_q might fluctuate in many orders in magnitude in the critical region [15] (these fluctuations are shown in Fig. 6), it is more convenient to study logarithm of I_q. Thus, our scaling variable is then defined as

$$Y_q(E) = \frac{1}{N_{\rm stat}} \sum_{i}^{N_s} \sum_{|E-E_n|<\delta} \ln I_q(E_n), \tag{4}$$

where $N_{\rm stat} = \sum_i n_i$. In our calculations, $N_{\rm stat} \sim 10^5$ (5×10^4 for $L \geq 50$) and $\delta = 0.025$. With these parameters, we calculate $Y_q(E)$ with relative accuracy better than 0.2%. Numerical data were collected by LAPACK subroutines for $L \leq 16$. For larger system size ($L \leq 54$) we use our own program based on the Lanczos algorithm.

We expect that Y_q is a good scaling variable, so that it behaves in the vicinity of the critical point as

$$Y_q(E, L) = Y_q^c - d_q \ln L + A(E - E_c)L^{1/\nu}, \tag{5}$$

for the fixed disorder W, and

$$Y_q(W, L) = Y_q^c - d_q \ln L + A(W - W_c)L^{1/\nu}, \tag{6}$$

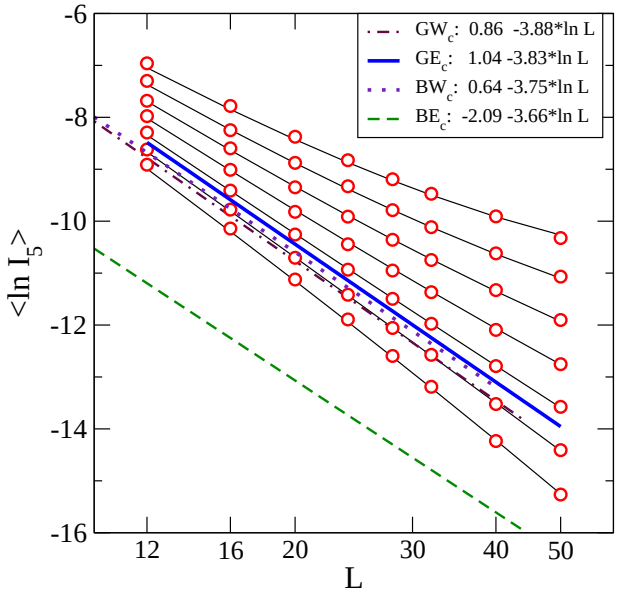

FIG. 2: (Color online) $Y_5(E, L)$ as a function of system size L for various energies $E = 6.50,\ 6.55,\ \ldots, 6.80$ (from bottom to top). Thin solid lines are fits, Eq. (5). Thick solid line is $\langle \ln I_5 \rangle = Y_5^c - 4\ d_5 \ln L$ (Eq. 7) for the critical energy $E_c \approx 6.58$. The same fit for other three critical points are also shown (described by legend). Data confirm universal L-dependence of Y_5 for three critical points. The different behavior for the critical point BE_c is due to strong finite-size effect, discussed in the text.

for the fixed energy $E = 0$.

For a given q, we fit obtained numerical data for Y_q to Eqs. (5) or (6). Obtained results are in Figs. 2, 3 and 4. Typical data for $q = 2$ and $q = 5$ are given in Table I.

Figure 2 shows the L-dependence of Y_5 for Gaussian disorder $W = 2$ and for energies close to the critical energy, $E_c \approx 6.58$. We see that at the critical point,

	q	E_c	W_c	ν	d_q	$L_{\rm min}$	$L_{\rm max}$
GW_c	2	0	6.14(3)	1.45(2)	1.28(2)	16	44
GW_c	5	0	6.07(4)	1.53(2)	0.97(8)	16	44
GE_c	2	6.59(1)	2	1.44(2)	1.28(4)	20	50
GE_c	5	6.58(3)	2	1.52(2)	0.96(5)	20	50
BW_c	2	0	16.70(10)	1.42(2)	1.23(7)	16	40
BW_c	5	0	16.53(10)	1.49(2)	0.93(9)	16	40
BE_c	2	7.44(2)	10	1.06(1)	1.11(8)	32	54
BE_c	5	7.43(3)	10	1.08(1)	0.87(32)	32	54

TABLE I: Critical exponent, ν, and fractal dimensions, d_q, calculated by scaling analysis of the inverse participation ratio, I_q, for four critical points. Calculated position of critical points, E_c, W_c, is given in the 3rd column. GW_c - Gaussian disorder, band center, GE_c - Gaussian disorder, band tail, BW_c - Box disorder, band center, BE_c - Box disorder, band tail. Data for system of the size $L_{\rm min} \leq L \leq L_{\rm max}$ were used in the scaling analysis.

$E = E_c$, $Y_q(E_c)$ decreases logarithmically,

$$Y_q(E_c, L) = Y_q^c - d_q \ln L, \qquad (7)$$

in agreement with Eq. (5). Outside the critical point, the L dependence of Y_q changes due to the presence of the term $\sim (E - E_c)L^{1/\nu}$. Similar analysis, performed for other critical points confirms the universality of the relationship (7). This indicates that parameters Y_q^c, d_q and A are universal.

There are two sources of inaccuracy of the scaling analysis: (i) if the critical region is not sufficiently narrow, then the linear term $\sim E - E_c$ could not be sufficient to describe a correct E-dependence of numerical data and higher order terms of the expansion (5) must be considered [5]. To test the accuracy of the linear approximation, we add also cubic term, $\sim (E-E_c)^3$ in Eq. (5). We found that such correction does not influence obtained critical parameters and might be neglected. (ii) for small system size, L, the variable Y_q suffers from finite-size effects (FSE) [5]. The role of FSE can be estimated by the scaling analysis for data of restricted system size, $L \geq L_{\min}$. For three critical points, GE_c, GW_c and BW_c (the position of critical points is given in Table I), we found that data for $L > L_{\min} \sim 16 - 20$ are already free of FSE. However, we were not able to obtain reliable critical parameters for the critical point BE_c. As shown in Table I and Fig. 2, our numerical data for this critical point are still far from limiting values. For this critical point we can only demonstrate the convergence of critical parameters to expected universal values when $L_{\min}$ increases (inset of Fig. 4). Larger samples are necessary to prove this convergence numerically.

Figure 3 summarizes our data for fractal dimensions, d_q. Data confirm that the spatial distribution of the wave function is universal, independent on the position of the critical point along the critical line. Presented data for d_q are in agreement with previously reported values [16].

Figure 4 presents obtained data for the critical exponent, ν. Wee see that ν converges to the generally accepted value, $\nu \sim 1.57$ [5, 6], when either $L_{\min}$ or q increases. In order to show the effect of the system size, we plot for each value of q a few data obtained with increasing minimal system size used in the scaling procedure. Inset of Fig. 4 presents our data for the critical point BE_c. Because of strong finite-size effects, much larger systems are necessary for the estimation of reliable values the critical exponent.

To understand the origin of the FSE, we calculated the density of states, $\rho(E)$, in the critical region of all four critical points. As shown in left Fig. 5, $\rho(E = 0)$ changes only in a few % when disorder varies around the critical value, W_c. Contrary to the band center, the density $\rho(E)$ around the mobility edge GE_c decreases significantly (almost by factor of two) in the critical region (right Fig. 5). In the case of critical point BE_c, this decrease is even more significant. Intuitively, one expects

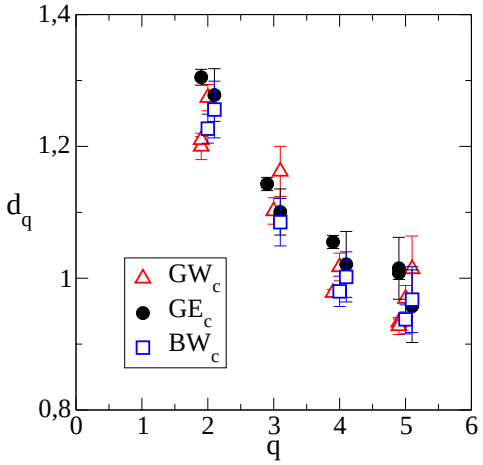

FIG. 3: (Color online) Fractal dimensions, d_q, calculated by scaling analysis of Y_q for three critical points. A small horizontal shift of symbols for a given q indicates minimal system size, $L_{\min}$, used in the scaling analysis: $L_{\min} = 8$ (left), 16 (middle) and 20 (right).

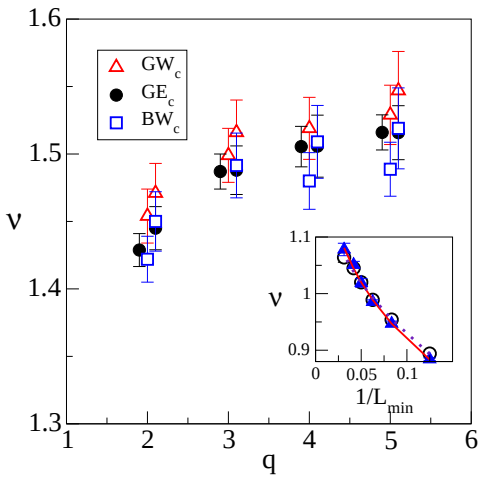

FIG. 4: (Color online) Critical exponent, ν, calculated from the scaling behavior of Y_q for three critical points. A small horizontal shift of symbols for a given q indicates minimal system size, $L_{\min}$, used in the scaling analysis: $L_{\min} = 8$ (left), 16 (middle) and 20 (right). Inset shows the critical exponent ν calculated for critical point BE_c from Y_2 (circles) and Y_5 (triangles). ν increases when data for smaller system size are omitted ($L_{\min}$ increases). This indicates that the deviation from universality, observed in this critical point, is only finite size effect. Solid (dashed) lines are fits $a_0 + a_1/L^{a_2}$ with $a_0 \approx 1.36$ (1.29) for $q = 5$ ($q = 2$), respectively.

that the one-parameter scaling works better when electronic states inside the critical region have the same, or at least comparable, density. Since the interval of energies, $\Delta E = 0.3$, used in the case of GE_c is already sufficient to get correct critical parameters, we expect that the the energy interval for BE_c must be $\Delta E \approx 0.2$. However, narrower interval of energies requires larger system

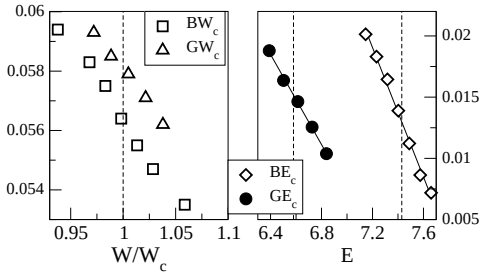

FIG. 5: The density of states, $\rho(E)$, arround the critical points. Dashed vertical lines indicates the position of critical points. Left: the disorder dependence of the density $\rho(E=0)$ at the band center. $\rho(E=0)$ changes only in 10% when disorder varies wihin the intervals ($15.5 \le W \le 17.5$ for BW_c and $6.5 \le W \le 6.8$ for GW_c) used our scaling analysis. Left: The density of states, $\rho(E)$ around the critical points GE_c and WE_c. Solid lines are linear fits with slopes 0.018 (GE_c) and 0.026 (BE_c).

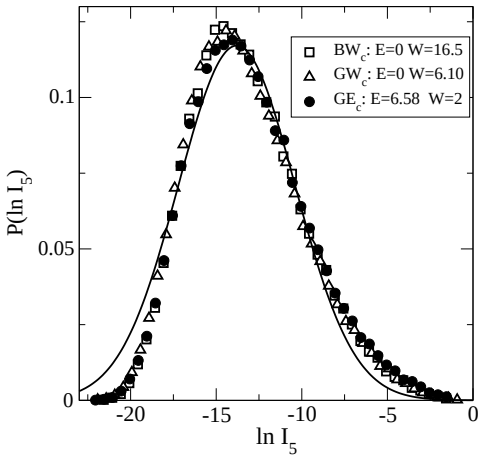

FIG. 6: Probability distribution $P(\ln I_5)$ for three critical points and $L = 40$. We used data from narrow energy interval, $E_c \pm \delta E$. The size of the system is $L = 40$. Note that neither mean value nor the distribution is system-size independent. Mean value, $\langle \ln I_5 \rangle = -13.08$. The value of the variance, $\mathrm{var} \ln I_5 = 11.6$, agrees with estimation of Ref. [16]. Solid line is Gaussian distribution with the same mean value and variance.

size. To have the term $(E - E_c)L^{1/\nu}$ of the same magnitude as in the GE_c-case, the size of the system must be $(3/2)\nu \approx 1.8$-times larger than in the GE_c case. Consequently, we expect that the scaling analysis of systems of the size $L_{\max} \approx 90-100$ would lead to correct estimation of the critical exponent also for the critical point BE_c.

We expect that I_q is less sensitive to finite size effects when q increases. Since the spatial distribution of electron is non-homogeneous in the critical regime, the main contribution to I_q is given by sites with large values of $|\Phi_n|$. Those sites are well localized in space and so insensitive to the system size. This is confirmed also by data shown in Fig. 4.

The universality of the spatial distribution of the critical wave function is confirmed also by Fig. 6 which shows the probability distribution of $\ln I_5$ for three critical points, GE_c, GW_c and BW_c. The width of the distribution, $\sigma_q = \sqrt{\mathrm{var} \ln I_q} \sim 3.4$, is close to the limiting value reported in Ref. [17]. However, the distribution $P(\ln I_q)$ is not system size invariant. The mean value of $\ln I_q$ decreases when system size increases, while the distribution always possesses a long tail for $\ln I_q \sim 1$ [17, 18, 19].

In conclusion, we investigated numerically the wave function of electron in the critical regime of the metal-insulator transition. By the scaling analysis of the logarithm of the inverse participation ratio, I_q, we calculated the critical exponent, ν, and fractal dimensions, d_q. We found that these parameters depend neither on the microscopic details of the disorder nor on the position of the critical point. This result confirms that the metal-insulator transition is universal along the critical line which separates metallic and insulating regimes.

This work was supported by grant APVV, project n. 51-003505 and VEGA, project n. 2/6069/26.

[1] E. Abrahams, P. W. Anderson, D. C. Licciardello, T. V. Ramakrishnan, Phys. Rev. Lett. **42**, 673 (1979)
[2] A. MacKinnon,B. Kramer, Phys. Rev. Lett. **47** 1546 (1981)
[3] A. MacKinnon, B. Kramer, Z. Phys. B **53**, 1 (1983)
[4] B. R. Bulka, B. Kramer, A. MacKinnon, Z. Phys. B **60**, 13 (1985)
[5] K. M. Slevin, T. Ohtsuki, Phys. Rev. Lett. **82**, 382 (1999)
[6] K. Slevin, P. Markoš, T. Ohtsuki, Phys. Rev. Lett. **86**, 3594 (2001)
[7] K. Slevin, P. Markoš, T. Ohtsuki, Phys. Rev. B **67**, 155106 (2003)
[8] B. I. Shklovskii, B. Shapiro, B. R. Sears, P. Lambrianides, B. H. Shore, Phys. Rev. B **47**, 11487 (1993)
[9] I. Kh. Zharekeshev, B. Kramer, Phys. Rev. B **51**, 17239 (1995)
[10] B. Kramer, K. Broderix, A. MacKinnon, M. Schreiber Physica A **167**, 163 (1990)
[11] P. Cain, R. A. Römer, M. Schreiber, Ann. Phys. (Leipzig) **8**, SI-33 (1999)
[12] A. Croy, R. A. Römer, physica status solidi c **3**, 334 (2006)
[13] B. Kramer, A. MacKinnon, Rep. Progr. Phys. **56** 1469 (1993)
[14] F. Evers, A. D. Mirlin, Phys. Rev.Lett. **84**, 3690 (2000)
[15] A. D. Mirlin, F. Evers, Phys. Rev. B **62**, 7920 (2000)
[16] A. Mildenberger, F. Evers, A. D. Mirlin, Phys. Rev. B **66**, 033109 (2002)
[17] F. Evers, A. Mildenberger, A. D. Mirlin, Phys. Rev. B **64**, 241303(R) (2001)
[18] E. Cuevas, Phys. Rev. B **66**, 233103 (2002)
[19] E. Cuevas, M. Ortuno, V. Gasparian, A. Perez-Garrido, Phys. Rev. Lett. **88**, 016401 (2002)